

Sonication Derived Powdered Mixtures of Ferrite and Ceramic Nanoparticles for H₂ Generation

Vinod S. Amar, Xavier M. Pasala, Jan A. Puszynski, Rajesh V. Shende *

Department of Chemical and Biological Engineering, South Dakota School of Mines and Technology, Rapid City, South Dakota, USA

*Corresponding author: Rajesh.Shende@sdsmt.edu

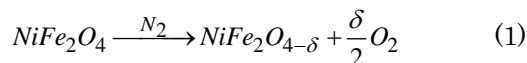
Abstract This paper reports sonication derived powdered mixtures of NiFe₂O₄ and ceramic nanoparticles such as ZrO₂/Y₂O₃/YSZ for H₂ generation from thermochemical water-splitting process. To prepare powdered mixtures, NiFe₂O₄ (75 wt%) and ceramic nanoparticles (25 wt%) were placed in ethanol, sonicated for 120 min, and the slurry obtained was dried at 50°-100°C. Using these powdered mixtures, ten consecutive thermochemical cycles were performed at 900°-1100°C for H₂ generation. Among different powdered mixtures, NiFe₂O₄/ZrO₂ produced a maximum H₂ of 30.6 mL/g/cycle at NTP conditions. Powdered mixtures prepared with different sonication times (30-120 min) and ZrO₂ nanoparticles loadings (10-35 wt%) were also investigated for H₂ generation *via* thermochemical water-splitting process. Sonication derived NiFe₂O₄/ZrO₂ powdered mixture prepared at optimized conditions has produced average H₂ volume of 38.8 mL/g/cycle during five consecutive thermochemical cycles, which was found to be higher than the H₂ volume generated by NiFe₂O₄/Y₂O₃ and NiFe₂O₄/YSZ powdered mixtures. In addition, these powdered mixtures were characterized for powdered x-ray diffraction (XRD), Brunauer-Emmett-Teller (BET) specific surface area, and scanning and transmission electron microscopy (SEM and TEM).

Keywords: thermochemical water-splitting, powdered mixtures, thermal stabilization, ultrasonication, sol-gel

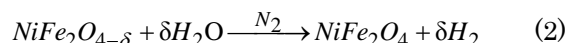
Cite This Article: Vinod S. Amar, Xavier M. Pasala, Jan A. Puszynski, and Rajesh V. Shende, "Sonication Derived Powdered Mixtures of Ferrite and Ceramic Nanoparticles for H₂ Generation." *American Journal of Energy Research*, vol. 3, no. 2 (2015): 25-31. doi: 10.12691/ajer-3-2-2.

1. Introduction

Solar thermal reactors utilizing SiC honeycomb support coated with the redox materials are being used for H₂ production from thermochemical water-splitting reaction [1]. This process involves two-steps where in step-1 (regeneration), ferrite (e.g. NiFe₂O₄) is partially reduced at elevated temperature of ~1100°C under constant N₂ flow conditions producing O₂.



In step-2 (water-splitting), partially reduced ferrite scavenges oxygen typically at lower temperatures (~900°C) generating H₂ as per the following reaction,



Together regeneration and water-splitting steps constitute one thermochemical cycle. As these steps are performed at different temperatures, the redox materials develop thermal stresses that lead to sintering or grain growth, which eventually cause spalling of redox materials in solar thermal reactors. This spalling can lead to significant pressure drop especially during the water-splitting step. Therefore, it is highly desirable to address the spalling issues in these reactors which can be achieved by employing thermally stable redox materials.

Thermally stable redox materials can be obtained by combining redox materials with refractory ceramics (e.g. ZrO₂, Y₂O₃, and YSZ) *via* powder mixing and core-shell synthesis routes. Vortex mixing [2] and sonication [3] techniques can be used to achieve powdered mixtures of redox and ceramic nanoparticles. It is anticipated that the higher thermal stability of ceramic particles can prevent the grain growth of the nanosized redox material in a powdered mixture. Such powdered mixtures can possibly be utilized in a thermal reactor to prevent spalling of redox material. A reduction in thermally induced spalling was observed by the addition of ZrO₂ in alumina bricks for the carbon black reactor [4]. Agrafiotis et al. [1] reported improved thermal and chemical stability of coating/support assembly in SiC monolith by the inclusion of YSZ (8 mol% Y₂O₃ in ZrO₂) intermediate layer. It is believed that this intermediate coating layer would mitigate grain boundary migration at the interface of redox material and the support. However, potential sintering or grain growth among the particles of redox material can still persist as YSZ layer is not segregating the individual particles of the redox materials.

Bhosale et al. [5,6,7] performed thermochemical water-splitting reaction for the H₂ generation using sol-gel derived NiFe₂O₄ [5], MnFe₂O₄ [6], and SnFe₂O₄ [7] nanoparticles with specific surface area (SSA) of 34-36.5 m²/g. These materials have shown significant grain growth and sintering after performing multiple thermochemical cycles in the temperature range of 900°-1100°C. For the NiFe₂O₄ material calcined at 600°C, the crystallite size was about 37 nm. After performing multiple thermochemical

cycles, the grain size was increased to few μm . This observation thus confirms the grain growth of redox nanoparticles. Furthermore the H_2 volume generated was found to decrease gradually with increase in thermochemical cycles [5]. Cheuh et al. [8] reported 500 thermochemical cycles using non-stoichiometric ceria where a similar trend of the reduction in H_2 volume with increase in number of thermochemical cycles can be observed. Thus, stable H_2 volume generation is difficult to achieve because of grain growth and sintering of redox nanoparticles during thermochemical water-splitting. Islam et al. [9] reported effects of sintering temperature on grain-growth and porosity of a ferrite material.

To address the grain growth issue, our research group has recently reported the powdered mixtures of sol-gel derived NiFe_2O_4 nanoparticles with thermally stable, ZrO_2 nanoparticles prepared via vortex mixing [2] and sonication [3] for H_2 generation from thermochemical water-splitting reaction. Bhosale et al. [2] performed thermochemical water splitting using a powdered mixture of $\text{NiFe}_2\text{O}_4/\text{ZrO}_2$ nanoparticles prepared via vortex mixing and reported 116.22, 35.63, 22.44 and 16.46 mL of H_2/g during 1st, 2nd, 3rd and 4th water-splitting step, respectively. At these reaction conditions, 100.04, 22.35, 13.65, and 9.63 mL of H_2/g was generated by NiFe_2O_4 nanoparticles over four consecutive thermochemical cycles performed at 900°-1100°C. These results indicate that the average volume of H_2 generated is higher for $\text{NiFe}_2\text{O}_4/\text{ZrO}_2$ powdered mixture. Furthermore, the SEM images of $\text{NiFe}_2\text{O}_4/\text{ZrO}_2$ powdered mixture indicated heterogeneous grain growth with fewer grains of 1-3 μm and many grains in the range of 200-500 nm, whereas the SEM images of NiFe_2O_4 showed increase in the grain size to 2-5 μm . Thus, the powdered mixture prepared by vortex mixing has mitigated the grain growth. However, as the heterogeneous grain growth was observed with the powdered mixture prepared via vortex mixing, Pasala et al. [3] recently reported H_2 generation from the thermochemical water-splitting reaction using $\text{NiFe}_2\text{O}_4/\text{ZrO}_2$ powdered mixture prepared via sonication. For this material, 124.32, 55.03, 50.36 and 30.69 mL of H_2/g was observed during 1st, 2nd, 3rd, and 4th cycle, respectively at the same water-splitting and regeneration temperatures of 900°-1100°C. The average H_2 volume generated during four consecutive thermochemical cycles was 64.6 mL of $\text{H}_2/\text{g}/\text{cycle}$ for the powdered mixture prepared using sonication, whereas 47.69 mL $\text{H}_2/\text{g}/\text{cycle}$ was observed with the powdered mixture prepared via vortex mixing. These results suggest that the sonication mixing has some advantages over vortex mixing in terms of mitigation of heterogeneous grain growth. Although the study reported by Pasala et al. [3] has shown higher H_2 generation presumably due to better dispersion of ferrite and ceramic nanoparticles in a powdered mixture, it does not include the effects of sonication time on the dispersion characteristics and the loading of ceramic nanoparticles in powdered mixtures on grain growth mitigation.

Thermal stabilization of the redox materials can be achieved by core-shell morphology where the redox material is enclosed in a porous shell of refractory ceramics such as ZrO_2 [10] and Y_2O_3 [11]. However achieving such morphology with ferrites can be often challenging [12] as they tend to form agglomerates due to their magnetic nature thereby resulting in incomplete

coverage of ceramic shell, and entrapment of impurities between the agglomerates and shell interface. Additionally, the presence of external ceramic layer on ferrites create an additional diffusion barrier [13,14] limiting the rate of water-splitting reaction.

In this study, NiFe_2O_4 nanoparticles were synthesized using the previously reported sol-gel method [5,10] and mixed with ceramic nanoparticles such as ZrO_2 , Y_2O_3 and YSZ via sonication performed in an ultrasonic bath. The sonication time was varied between 30-120 min and the optimum sonication time was deduced from settling experiments. Powdered mixtures were prepared with different ZrO_2 loading. Finally, H_2 generation ability of different powdered mixtures was investigated and compared with NiFe_2O_4 nanoparticles by performing multiple thermochemical cycles at 900°-1100°C.

2. Experimental

2.1. Materials

Nickel chloride hexahydrate ($\text{NiCl}_2 \cdot 6\text{H}_2\text{O}$), iron chloride tetrahydrate ($\text{FeCl}_2 \cdot 4\text{H}_2\text{O}$), and propylene oxide ($\text{C}_3\text{H}_6\text{O}$, 99%) were purchased from Alfa Aesar. Yttrium oxide (yttria, 30 – 50 nm, SSA: 27.5 m^2/g), zirconium oxide (zirconia, 20 – 50 nm, SSA: 40 m^2/g), and 8 mol% yttria stabilized zirconia (YSZ, 30 – 60 nm, SSA: 27.5 m^2/g) were purchased from Inframat Advanced Materials, USA. Quartz wool as a support for packing the powdered material in the reactor was purchased from Wale Apparatus Co. Inc., USA. Ceramic Raschig rings as a support material was purchased from Brewhaus, USA. N_2 from a gas cylinder with a minimum stated purity of 99.99% was purchased from Linweld Inc., USA. De-ionized water was used for steam generation.

2.2.1. Synthesis of Ni-ferrite nanoparticles: Ni-ferrite nanoparticles were synthesized using the previously reported sol-gel method [5,10].

2.2.2. Preparation of Ni-ferrite based powdered mixtures: Sol-gel derived Ni-ferrite was mixed with $\text{ZrO}_2/\text{Y}_2\text{O}_3/\text{YSZ}$ nanoparticles via sonication that was carried out in Branson 2510 ultrasonic bath (80 W, 40 kHz). Ferrite (5g) and ceramic nanoparticles (10-35wt%) were taken in a borosilicate glass vial containing ethanol (50 mL) and sonicated for 30 to 120 min. While sonication was in progress, the temperature of ultrasonic bath was maintained at 30°C. The resultant powdered slurry was initially dried overnight at 50°C and later at 100°C for 1 hour. The synthesis method used for Ni-ferrite and preparation of powdered mixtures are outlined in Figure 1.

2.3. Characterization of Powdered Mixtures

The specific surface area of the powdered mixtures was determined using BET (Brunauer-Emmett-Teller) surface area analyzer (Gemini II-2375 from Micromeritics). The sample was degassed in order to remove any contaminants prior to BET surface area analysis. The phase composition of powdered mixtures containing ferrite and ceramic nanoparticles was analyzed using Rigaku Ultima-Plus X-ray diffractometer ($\text{CuK}\alpha$ radiation, $\lambda=1.5406 \text{ \AA}$, 40 kV, 40 mA). The parameters such as 2θ , scanning speed and width of $10^\circ \leq 2\theta \leq 70^\circ$, 2° per minute and 0.020° ,

respectively, were used for the X-ray diffraction measurements. MDI Jade software was used for the analysis of diffraction patterns. Scanning electron microscopy/energy dispersive X-ray (EDX) spectroscopy

was performed using the Zeiss Supra 40 VP field emission SEM. The morphology and size of the nanoparticles in the powdered mixture was investigated by transmission electron microscopy (TEM) using JEOL 2100 HRTEM.

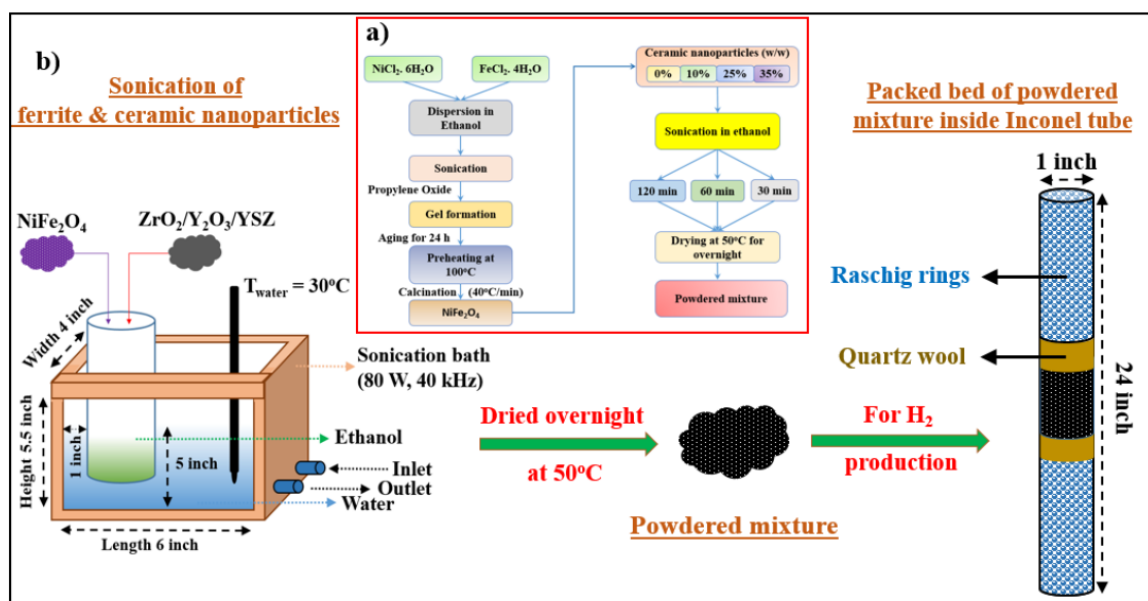


Figure 1. a) Preparation of NiFe₂O₄ nanoparticles and powdered mixtures, and b) schematic of sonication derived powdered mixture and its loading in an Inconel tubular reactor as a packed bed for thermochemical water-splitting

2.4. H₂ Generation Set-up and Thermochemical Water-Splitting Procedure

The hydrogen generation ability of the powdered mixture was examined using a high temperature thermochemical water-splitting reactor set-up reported elsewhere [11]. 5 g of powdered mixture was loaded inside the Inconel tubular reactor (from California Metal Inc.) supported by raschig rings forming a packed bed as shown in Figure 1. A vertical split furnace (from Carbolite, USA) was used around the Inconel reactor to achieve higher temperatures. A horizontal tube furnace (from Carbolite, USA) provided with a stainless steel tube was

used to vaporize the water. Deionized water from the reservoir was vaporized at 500°C through horizontal furnace and fed to reactor at constant flow rate of 1 mL/min. N₂ at the flow rate of 35 SCCM was used as a carrier gas. The exit gas stream from reactor was continuously monitored using an online H₂ sensor (H2scan) and the data acquisition was performed using a computer interfaced with the sensor. Further details can be found elsewhere [11].

Multiple thermochemical water-splitting cycles were performed at regeneration temperature of 1100°C and water-splitting temperature of 900°C. During the regeneration step at 1100°C, the powdered mixtures packed in the Inconel tubular reactor were partially reduced for an arbitrary time of 2 hours. Subsequently the water-splitting step was performed at 900°C for H₂ generation.

3. Results and Discussion

3.1. X-ray Diffraction of Ni-ferrite and Powdered Mixtures

Sol-gel derived Ni-ferrite and its powdered mixtures with ZrO₂/Y₂O₃/YSZ ceramic nanoparticles was characterized using XRD and their profiles obtained are shown in Figure 2. The 2θ peak positions of 18.52, 30.44, 35.8, 37.5, 43.4, 53.84, 57.44, and 63.12 suggest nominally phase pure composition of NiFe₂O₄ and found consistent with those reported elsewhere [5,15,16,17]. These 2θ reflections are denoted by ‘●’ in a powdered mixture. For a powdered mixture, 2θ reflections corresponding to 24.08, 28.2, 31.48, 40.8, 41.2, 49.32, 50.14, 50.58, 54.08, 59.82, 62.07, 64 (as shown by ‘◆’) reveals monoclinic phase for ZrO₂. The 2θ reflections of 23.71, 31.54, 33.78, 35.90, 39.84, 41.69, 48.53, 50.12, 54.7, 59.03, 60.43, 64.52 as denoted by ‘■’ suggests cubic Y₂O₃. For powdered mixture of NiFe₂O₄/YSZ, the major 2θ reflections (30.08, 34.94, 50.16, 59.62, 62.42) corresponding to tetragonal phase of YSZ are shown by ‘▲’. All the 2θ reflections corresponding to ZrO₂/Y₂O₃/YSZ are consistent with the standard ICDD patterns as reported in the standard literature [18,19,20].

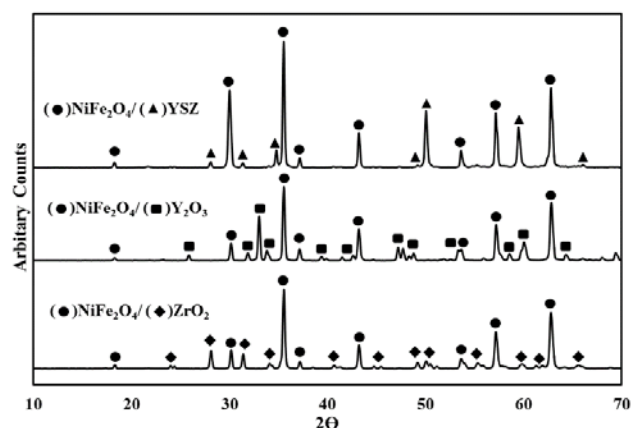


Figure 2. XRD patterns of powdered mixtures containing NiFe₂O₄ (75 wt%) and ZrO₂/Y₂O₃/YSZ (25 wt%)

3.2. BET Analysis of NiFe₂O₄ Powdered Mixtures

The BET specific surface area (SSA) of sol-gel derived NiFe₂O₄ powder was 35.55 m²/g. NiFe₂O₄ powder was mixed with ceramic nanoparticles (25wt% loading) as per the procedure described earlier in section 2.3 and the SSA of the powdered mixtures are presented in Table 1.

Table 1. BET SSA of the NiFe₂O₄ and powdered mixtures

Redox Material	Specific Surface Area (SSA) m ² /g
NiFe ₂ O ₄	35.55
NiFe ₂ O ₄ /ZrO ₂	33.70
NiFe ₂ O ₄ /YSZ	28.69
NiFe ₂ O ₄ /Y ₂ O ₃	31.00

3.3. Microstructural Characterization of NiFe₂O₄ mixed with ZrO₂, Y₂O₃ and YSZ

The SEM and EDX images of NiFe₂O₄/ZrO₂, NiFe₂O₄/Y₂O₃, and NiFe₂O₄/YSZ powdered mixtures are shown in Figure 3a-b, 3c-d and 3e-f, respectively. The SEM images show amorphous morphology whereas EDX mapping exhibit the distribution of ZrO₂, Y₂O₃ and YSZ nanoparticles in powdered mixtures. The nanoparticle morphology in the powdered mixtures was further studied using TEM as shown in Figure 4. From the particle size distribution as presented in Figure 4d, the average particle size was found to be in the range of 20-32 nm.

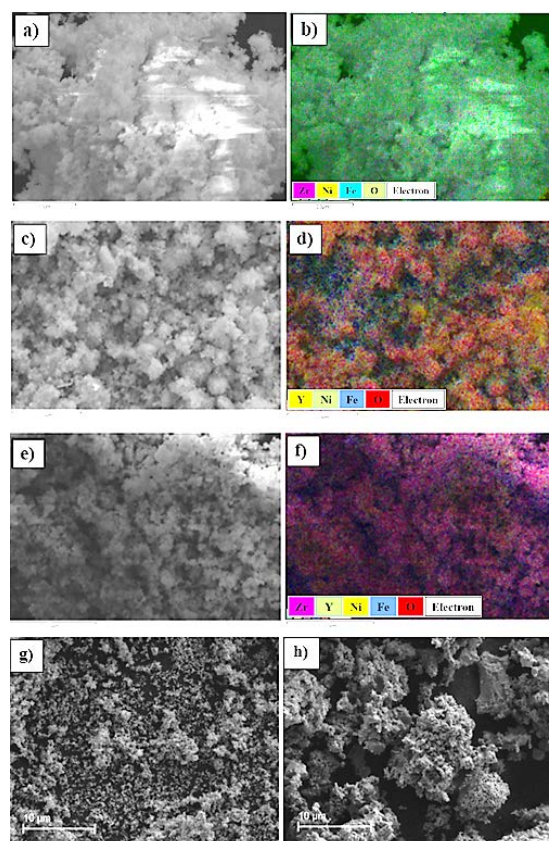


Figure 3. SEM and EDX mapping of powdered mixtures of NiFe₂O₄ with ZrO₂ (a, b), Y₂O₃ (c, d) and YSZ (e, f) and SEM of optimized NiFe₂O₄/ZrO₂ powdered mixture before reaction (g), and after reaction (h)

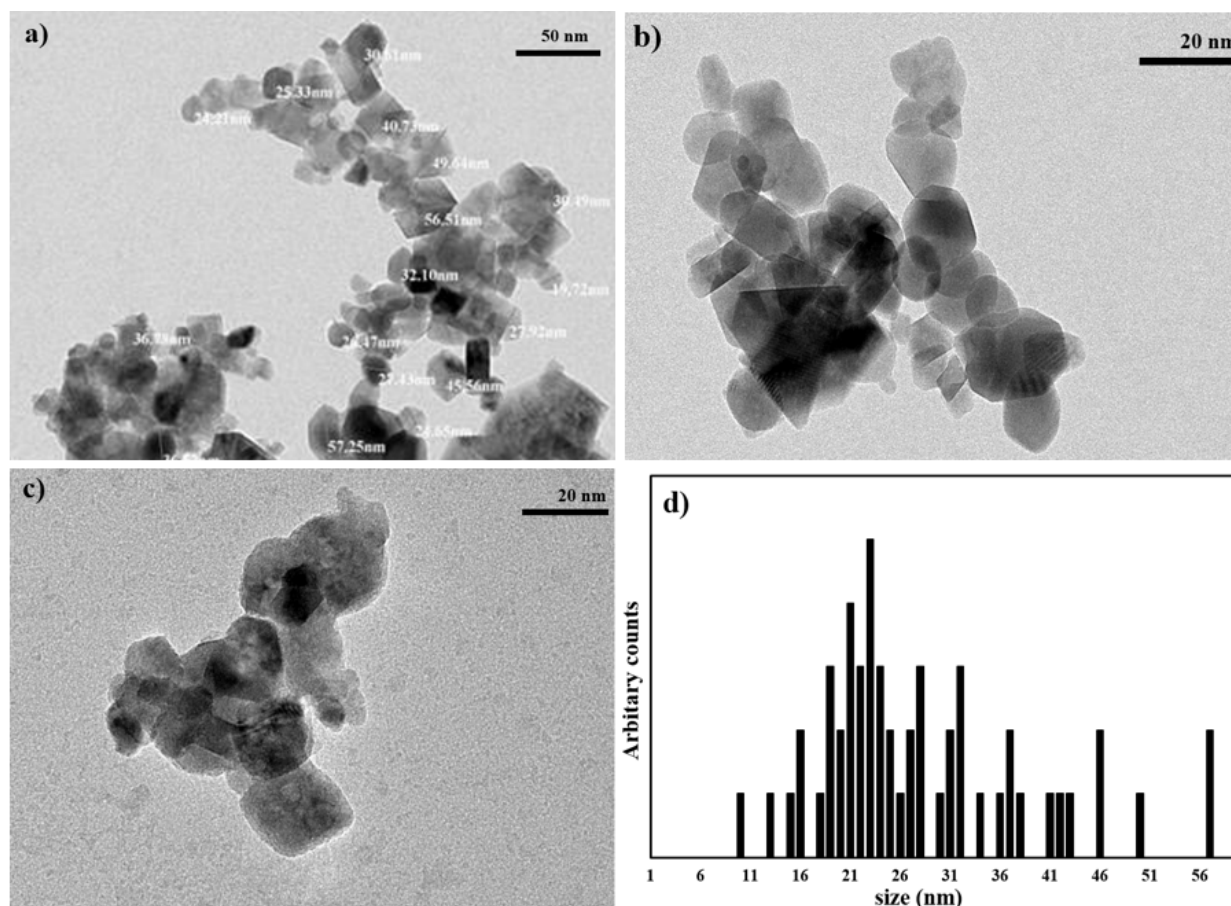


Figure 4. TEM images of sonication derived a) NiFe₂O₄/ZrO₂, b) NiFe₂O₄/YSZ c) NiFe₂O₄/Y₂O₃ powdered mixtures and d) particle size distribution inferred from all TEM images (a-c)

3.4. H₂ Generation Ability of Powdered Mixtures

NiFe₂O₄ and its powdered mixtures were individually loaded in Inconel tubular reactor. Their H₂ generation ability was investigated by performing ten consecutive thermochemical cycles, where water-splitting step was performed at 900°C and the regeneration step was carried out at 1100°C for 2 hours. The H₂ volumes produced at NTP conditions during ten consecutive thermochemical cycles are summarized in Table 2. The results indicate higher H₂ volume generation using NiFe₂O₄/ZrO₂ as compared to other powdered mixtures prepared with Y₂O₃ and YSZ. Therefore, NiFe₂O₄/ZrO₂ was further considered to investigate the effects of sonication time and ZrO₂ loading in a powder mixture on H₂ production via thermochemical water-splitting reaction.

Table 2. H₂ volume (mL/g) generated by NiFe₂O₄ and Ni-ferrite powdered mixtures during ten consecutive thermochemical cycles

Cycle	NiFe ₂ O ₄	H ₂ mL/g at NTP		
		NiFe ₂ O ₄ mixed with		
		ZrO ₂	YSZ	Y ₂ O ₃
1	100.04	124.32	18.74	15.47
2	22.35	53.46	14.41	4.32
3	13.64	50.36	6.35	3.33
4	9.63	30.69	4.41	3.37
5	4.98	7.83	8.09	2.78
6	6.39	7.84	3.70	3.11
7	7.64	10.23	3.35	2.65
8	3.81	7.34	6.55	1.89
9	2.94	9.21	2.19	1.30
10	2.79	4.97	2.49	0.94
Avg. H ₂	17.42	30.58	7.02	3.91

3.4.1. Effect of Ultrasonication Time on Dispersion Settling Characteristics and H₂ Generation

The effect of ultrasonication time on the dispersion settling characteristics was studied using NiFe₂O₄ (75wt%)/ZrO₂ (25wt%) powdered mixture. 1.0 g of the powdered mixture was placed in 40 mL ethanol and sonicated at three different sonication times of 30 min, 60 min and 120 min. The resultant dispersion was taken in a measuring cylinder and left for 12 hours to observe settling. Throughout the settling study, the measuring cylinder was covered with Parafilm to prevent the evaporation of ethanol (vapor pressure at 25°C is 0.07922 bar [21]) and to prevent contamination of the dispersion with airborne dust/impurities. After 12 hours, the dispersion prepared with 60 min sonication time was found to have lowest settling velocity of 0.009 cm/min as compared to the other dispersions prepared with sonication times of 30 min and 120 min (Figure 5). Higher settling velocity for a dispersion prepared with 120 min could be due to sintering of nanoparticles. As the sonication time increases, the intensity of hotspots increases that can raise the temperature and lead to sintering [22].

In general, ultrasonic irradiation into suspension of submicron or nanoparticles is effective in eliminating the agglomeration. Ultrasonic irradiation into a suspension or

a liquid result in alternating high-pressure and low pressure cycles that apply mechanical stresses to overcome the weak attractive forces exist between the particles leading to better dispersion characteristics [23]. In addition, the ultrasonic cavitation in liquid causes high speed liquid jets that are responsible for effective means of dispersion and deagglomeration of the particles [24,25]. If particles are not agglomerated their settling velocity can be easily determined using Stokes law [26]. However, due to the magnetic nature of ferrites, agglomeration of the particles is difficult to avoid. Therefore, settling velocity of the dispersions was determined and presented in Figure 5.

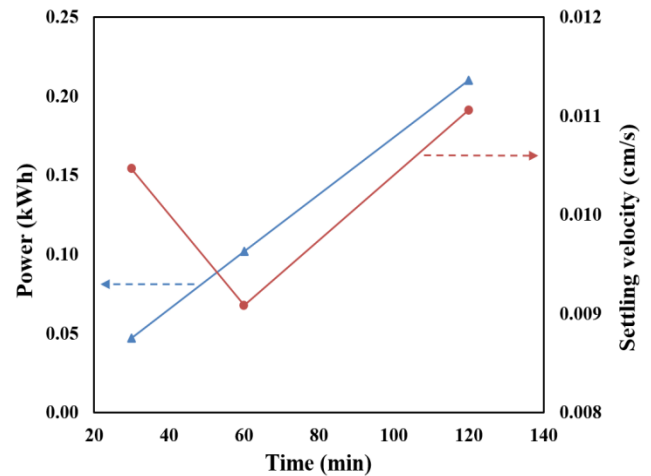


Figure 5. Power consumed and observed settling velocity for the dispersions as function of ultrasonication time

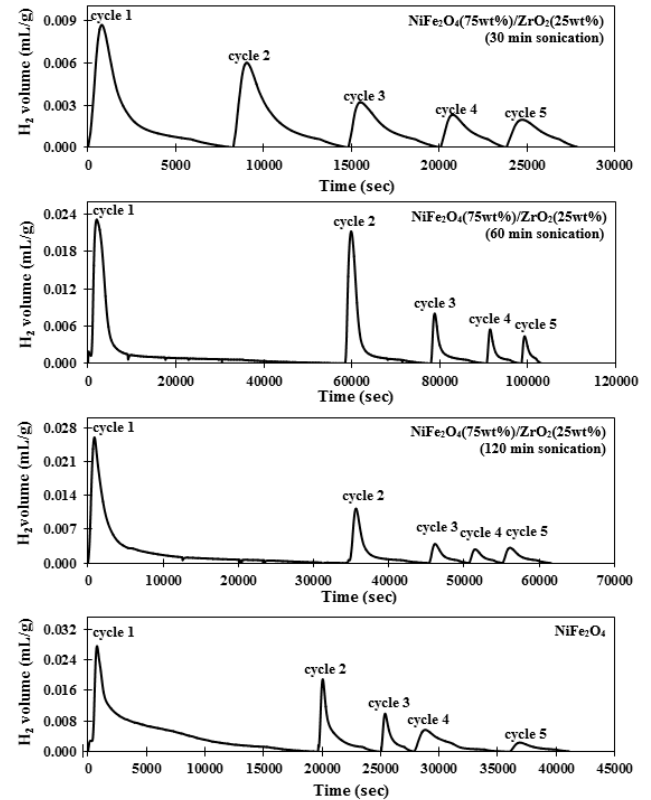


Figure 6. Transient hydrogen profiles obtained during five thermochemical cycles where water-splitting and regeneration steps were performed at 900°C and 1100°C, respectively using NiFe₂O₄ nanoparticles and NiFe₂O₄/ZrO₂ powdered mixtures prepared at different sonication times

Powdered mixtures of $\text{NiFe}_2\text{O}_4(75\text{wt}\%)/\text{ZrO}_2(25\text{wt}\%)$ were prepared at different sonication times of 30-120 min and loaded inside the Inconel reactor. Five consecutive thermochemical cycles were performed at water-splitting and regeneration temperatures of 900°C and 1100°C , respectively. The transient H_2 profiles obtained are shown in Figure 6 whereas the integrated H_2 volumes are presented in Figure 7. Maximum H_2 volume generation was observed with $\text{NiFe}_2\text{O}_4/\text{ZrO}_2$ powdered mixture prepared at the sonication time of 60 min, which was also found to be higher than NiFe_2O_4 nanoparticles.

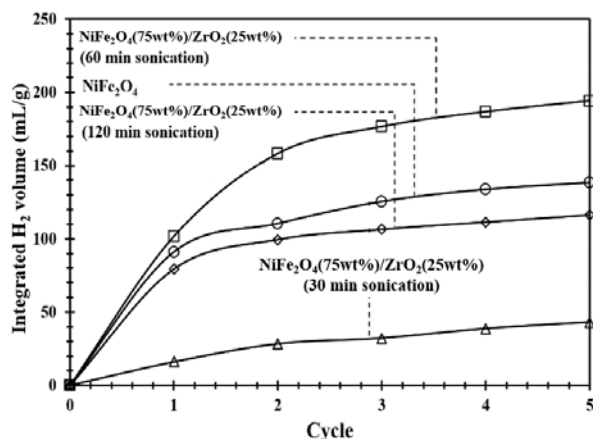


Figure 7. Integrated H_2 volume generated by NiFe_2O_4 and $\text{NiFe}_2\text{O}_4/\text{ZrO}_2$ powdered mixture prepared at different sonication times at water-splitting and regeneration temperatures of 900°C and 1100°C , respectively

These results suggest inhibition of the grain growth of NiFe_2O_4 nanoparticles in the presence of refractory ZrO_2 nanoparticles that presumably reflected into higher H_2 volume generation.

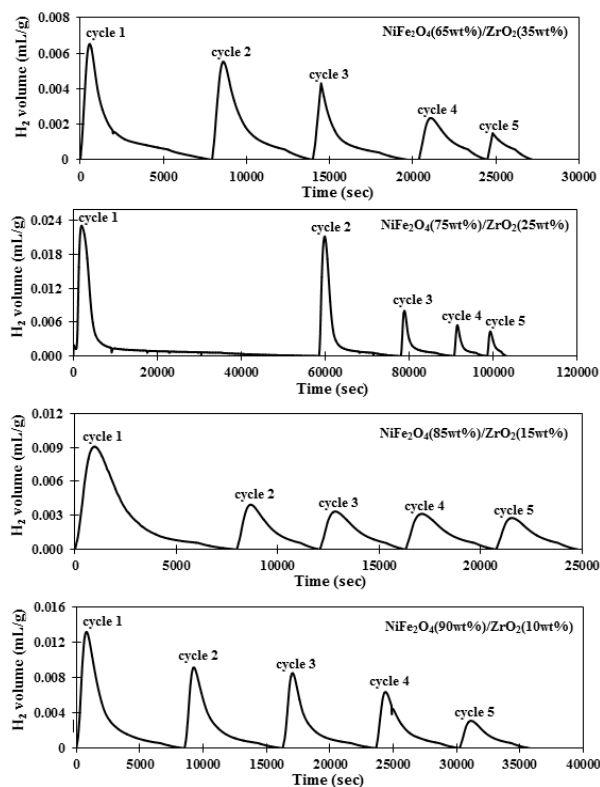


Figure 8. Transient hydrogen profiles obtained during five thermochemical cycles where water-splitting and regeneration steps were performed at 900°C and 1100°C , respectively using $\text{NiFe}_2\text{O}_4/\text{ZrO}_2$ powdered mixtures prepared using optimized sonication time of 60 min

3.4.2. Effect of ZrO_2 Loading in a Powdered Mixture on Hydrogen Generation

At optimum sonication time of 60 min, powdered mixtures of $\text{NiFe}_2\text{O}_4/\text{ZrO}_2$ were prepared using different ZrO_2 loadings of 10-35 wt%. Using these powdered mixtures, five consecutive thermochemical cycles were performed at water-splitting and regeneration temperatures of 900°C and 1100°C , respectively and the transient H_2 profiles obtained are shown in Figure 8, whereas the integrated H_2 volumes are presented in Figure 9. Maximum H_2 volume was observed for $\text{NiFe}_2\text{O}_4(75\text{wt}\%)/\text{ZrO}_2(25\text{wt}\%)$ powdered mixture as compared with the powdered mixtures prepared with ZrO_2 loadings of 10 wt%, 15 wt% and 35 wt%. Higher H_2 volume observed with the powdered mixture suggest grain growth mitigation of NiFe_2O_4 nanoparticles in the presence of ZrO_2 nanoparticles. The SEM images presented in Figure 4g-h, provide evidence of grain growth mitigation or thermal stabilization of NiFe_2O_4 nanoparticles by the addition of refractory ceramic nanoparticles. Further grain growth mitigation or thermal stabilization of redox material may be possible by the immobilization of ferrite nanoparticles on the ceramic monolithic structures. Currently, we are investigating the effect of immobilization on H_2 generation.

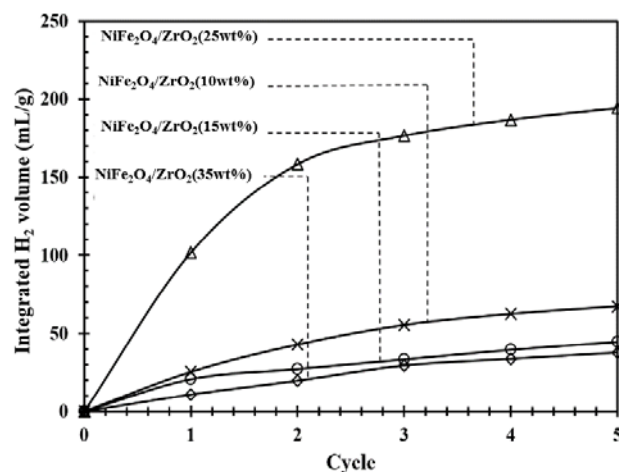


Figure 9. Integrated H_2 volume generated by the powdered mixtures prepared at different ZrO_2 loadings and optimized sonication time of 60 min at water-splitting and regeneration temperature of 900°C and 1100°C

4. Conclusions

Powdered mixtures of NiFe_2O_4 and ceramic (ZrO_2 , Y_2O_3 and YSZ) nanoparticles were prepared by ultrasonication and their ability towards H_2 generation via thermochemical water-splitting process was investigated. Average H_2 volume of 30.6 mL/g/cycle, 3.9 mL/g/cycle and 7 mL/g/cycle generated by $\text{NiFe}_2\text{O}_4/\text{ZrO}_2$, $\text{NiFe}_2\text{O}_4/\text{Y}_2\text{O}_3$ and $\text{NiFe}_2\text{O}_4/\text{YSZ}$, respectively at 900°C and 1100°C during ten consecutive thermochemical cycles. As maximum H_2 volume generation was observed with $\text{NiFe}_2\text{O}_4/\text{ZrO}_2$, this powdered mixture was optimized with respect to the ultrasonication time and ZrO_2 loadings. At optimized ultrasonication time of 60 min and ZrO_2 loading of 25 wt%, average H_2 volume of 38.8 mL/cycle/g was observed during five consecutive thermochemical cycles at water-splitting and regeneration temperature of 900°C and 1100°C , respectively, which

was found to be higher than the H₂ volume generated by the other powdered mixtures as well as NiFe₂O₄ nanoparticles. These results suggest that the grain growth of NiFe₂O₄ nanoparticles has been mitigated in the presence of ceramic nanoparticles, which was evident in the SEM images. Thus, thermal stabilization of ferrite nanoparticles could be achieved by the addition of refractory ceramic nanoparticles.

Acknowledgements

The authors gratefully acknowledge the financial support from the National Science Foundation, grant number CBET#1134570, and Chemical and Biological Engineering department at South Dakota School of Mines & Technology.

References

- [1] Agrafiotis, C., Pagkoura, C., Lorentzou, S., Kostoglou, M., and Konstandopoulos, A., "Hydrogen production from solar reactors," *Catalysis Today*, 127[1-4], 265-277, September 2007.
- [2] Bhosale, R.R., Puszynski, J.A., and Shende, R.V., "Sol-gel derived NiFe₂O₄ modified with ZrO₂ for hydrogen generation from solar thermochemical water-splitting reaction," in *MRS Proceedings*, Vol. 1387, Cambridge University Press, 2012.
- [3] Pasala, X., Bhosale, R.R., Amar, V.S., Puszynski, J.A., and Shende, R.V., "Thermally stabilized ferrite nanoparticles for hydrogen generation from thermochemical water-splitting reaction," in *Proceedings of AIChE Annual Meeting*, 2012.
- [4] Bhowmick, T., "A study on the development of refractories for carbon black reactor," M.Tech. Thesis in Ceramic Engineering, National Institute of Technology, Rourkela, 2013.
- [5] Bhosale, R.R., Shende, R.V., and Puszynski, J.A., "H₂ generation from thermochemical water-splitting using sol-gel derived Ni-ferrite," *Journal of Energy and Power Engineering*, 4(6), 27-38, June 2010.
- [6] Bhosale, R.R., Shende, R.V., and Puszynski, J.A., "Thermochemical water-splitting for H₂ generation using sol-gel derived Mn-ferrite in a packed bed reactor," *International Journal of Hydrogen Energy*, 37(3), 2924-2934, February 2012.
- [7] Bhosale, R.R., Khadka, R.P., Puszynski, J.A., and Shende R.V., "H₂ generation from two-step thermochemical water-splitting reaction using sol-gel derived Sn_xFe_yO_z," *Journal of Renewable and Sustainable Energy*, 3(6), 063104, November 2011.
- [8] Chueh, W.C., Falter, C., Abbott, M., Scipio, D., Furler, P., Haile, S.M., and Steinfeld, A., "High-flux solar-driven thermochemical dissociation of CO₂ and H₂O using nonstoichiometric ceria," *Science*, 330(6012), 1797-1801, December 2010.
- [9] Islam, R., Rahman, M.O., Hakim, M.A., Saduzzaman, S., Noor, S., and Al-Mamun, M., "Effect of Sintering Temperature on structural and magnetic properties of Ni_{0.55}Zn_{0.45}Fe₂O₄ ferrites," *Materials Sciences and Applications*, 3, 326-331, February 2012.
- [10] Amar, V. S., Puszynski, J.A., and Shende, R.V., "Hydrogen generation from thermochemical water-splitting using core shell Ni-ferrite nanoparticles," in *Cleantech Proceedings*, 139-142, 2014.
- [11] Amar, V. S., Puszynski, J.A., and Shende, R.V., "H₂ generation from thermochemical water-splitting using yttria stabilized NiFe₂O₄ core-shell nanoparticles," *Journal of Renewable and Sustainable Energy*, 7(2), 023113, March 2015.
- [12] Ghosh Chaudhuri, R, and Paria, S, "Core/shell nanoparticles: classes, properties, synthesis mechanisms, characterization, and application," *Chemical Reviews*, 112(4), 2373-2433, April 2012.
- [13] Scharlt, W., "Current directions in core-shell nanoparticle design," *Nanoscale*, 2, 829-843, March 2010.
- [14] Ballauff, M., and Lu, Y., "Smart nanoparticles: preparation, characterization and application," *Polymer*, 48(7), 1815-1823, March 2007.
- [15] Bhosale, R.R., "Thermochemical water-splitting for hydrogen generation using sol-gel derived ferrites." Ph.D. thesis in Chemical and Biological Engineering, South Dakota School of Mines and Technology, Rapid City, South Dakota, 2012.
- [16] Šepelák, V., Bergmann, I., Feldhof, A., Heitjans, P., Krumeich, F., Menzel, D., Litterst, F.J., Cambell, S.J., and Becker, K.D., "Nanocrystalline nickel ferrite, NiFe₂O₄: mechanosynthesis, nonequilibrium cation distribution, canted spin arrangement, and magnetic behavior," *The Journal of Physical Chemistry C*, 111, 5026-5033 March 2007.
- [17] Fresno, F., Fernández-Saavedra, R., Belén Gómez-Mancebo, M., Vidal, A., Sánchez, M., Isabel Rucandio, M., Quejido, A.J., and Romero, M., "Solar hydrogen production by two-step thermochemical cycles: evaluation of the activity of commercial ferrites," *International Journal of Hydrogen Energy* 34(7), 2918-2924, April 2009.
- [18] Gualtieri, A., Norby, P., Hanson, J., and Hriljac, J., "Rietveld refinement using synchrotron X-ray-powder diffraction data collected in transmission geometry using an imaging-plate detector – application to standard M-ZrO₂," *Journal of Applied Crystallography*, 29(6), 707-713, December 1996.
- [19] Paton, M.G., and Maslen, E.N., "A refinement of the crystal structure of yttria," *Acta Crystallographica*, 19, 307, December 1965.
- [20] Wang, D.N., Guo, Y.Q., Liang, K.M., and Tao, K., *Science in China Series A-Mathematics Physics Astronomy and Technological Sciences*, 42, 80, 1999.
- [21] Thompson, G.W., "The Antonie equation for vapor-pressure data," *Chemical Reviews*, 38(1), 1-39, February 1946.
- [22] Suslick, K.S., "The chemical effects of ultrasound," *Scientific American*, 260(2), 80-86, February 1989.
- [23] Sato, K., Li, J.G., Kamiya, H., and Ishigaki, T., "Ultrasonic dispersion of TiO₂ nanoparticles in aqueous suspension," *Journal of the American Ceramic Society*, 91(8), 2481-2487, July 2008.
- [24] Stephan, J. D., and Suslick, K.S., "Interparticle collisions driven by ultrasound," *Science*, 247, 1067-1069, March 1990.
- [25] Suslick, K.S., Didenko, Y., Ming, M.F., Taeghwan, H., Kenneth, J.K., William, B, Mc. Millan, M.M., and Mike, W., "Acoustic cavitation and its chemical consequences," *Philosophical Transactions of the Royal Society of London A: Mathematical, Physical and Engineering Sciences*, 357(1751), 335-353, February 1999.
- [26] Dietrich, W.E., "Settling velocity of natural particles," *Water Resources Research*, 18(6), 1615-1626, December 1982.